Indian J. Phys. **71A** (2), 117–130 (1997)

IJP A
— an international journal

Anisotropy in elastic wave propagation in selected high T_C superconductors

M S Kala and J Philip

Department of Physics & Instrumentation, Cochin University of Science & Technology, Cochin-682 022, India

Received 28 March 1996, accepted 19 September 1996

Abstract : In this paper, an attempt is made to study the anisotropy in elastic wave propagation in selected high T_c superconducting samples. Three systems have been investigated – $Bi_2Sr_2CaCu_2O_{8-\delta}$, $RBa_2Cu_3O_{7-\delta}$ (R = Y or Gd) and $La_{2-x}Sr_xCuO_{4-\delta}$ – for which the phase velocity surfaces are computed and plotted after solving the wave equations corresponding to different modes of propagation. The wave surfaces are plotted at temperatures above and below T_c, either for single crystals, sinterforged samples or ceramic polycrystalline specimens subject to the availability of elastic constant data. A detailed analysis of elastic wave surfaces and anisotropy in high T_c superconductors above and below T_c has been undertaken. A comparison of the wave velocity surfaces of the different materials suggest that the anisotropy in elastic wave propagation is not the same for these materials. An explanation for this, based on its structure, is provided. It is also found that the nature of elastic anisotropy does not vary significantly with superconducting transition.

Keywords : High T_c superconductors, elastic anisotropy, elastic wave propagation

PACS Nos. : 62.20.Dc, 74.90.+n

1. Introduction

The elastic properties of a material determine a number of fundamental solid state parameters such as phonon dispersion, specific heat, Debye temperature, thermal expansion, Gruneisen parameter *etc*. By measuring the phase velocities of elastic waves propagating along various crystallographic directions, the elastic constants of a material can be obtained. The relations between the elastic constants and the phase velocities in any arbitrary direction of a medium are obtained from a solution of the Christoffel equation [1].

Elastic wave propagation is highly anisotropic in many crystals in the sense that waves with different polarizations propagate with different velocities in different directions. Except for certain special directions, waves are not strictly transverse or longitudinal in crystals. The group velocity of the waves with which energy is transported is generally

different, both in direction as well as in magnitude from phase velocity. The phase and group velocities can be plotted for different propagation directions lying in different planes for each polarization mode which give the corresponding velocity and ray surfaces. The inverse of phase velocities can also be plotted for various propagation directions which are referred to as slowness surfaces. The pictorial representation of the wave velocities give a much better understanding of the anisotropic nature of elastic wave propagation in different directions in a crystal.

Measurement of the elastic constants of superconductors is very important since they have linkage to the superconducting transition temperature through the Debye temperature and the electron-phonon coupling parameter. In addition, the elastic constants directly determine the behaviour of long-wavelength acoustic phonons and provide a sensitive probe of structure related phase transitions occurring in these materials. Because of these reasons there have been a large number of studies on the elastic properties of these materials, particularly high T_c superconductors, with the aim of providing some insight into the mechanisms responsible for superconductivity.

Extensive sound velocity measurements have been made in high T_c superconducting cuprates for a variety of reasons. Firstly, as is obvious from their structures, they are extremely anisotropic structurally, with a strong two-dimensional character. Therefore, the relation of superconductivity to structural distortions could also be highly direction dependent. Measurement of the sound velocity anomaly at the superconducting transition for sound waves with different polarizations propagating in different directions would, in principle, provide information on this particular aspect of superconductivity. Secondly, there are structural transitions in these systems, such as tetragonal to orthorhombic, that occur above T_c which get reflected in elastic properties.

Most of the early work on the elastic properties of these materials were performed on ceramic polycrystalline samples using ultrasonic or vibrating reed technique. Since the synthesis of ceramic samples with dimensions large enough for ultrasonic measurements is comparatively easy, a number of papers have appeared in literature reporting elastic constants of such samples. Though these measurements provide a very good tool to probe the bulk properties of these materials, they fail to give information about elastic anisotropy, since such experiments generally probe the spherically averaged properties or the sample is treated as elastically isotropic.

Elastic constant measurements on single crystals is the answer to the above problem. The growth of single crystals of high T_c materials is not very easy, but people have succeded in recent years. Single crystals are usually in the form of thin platelets that do not allow the determination of the whole set of elastic constants and because of their small dimensions, precise measurement of elastic constants is rather difficult. Even by using the resonant ultrasound technique, which enables one to measure the elastic constants of small crystals, all the elastic constants of high T_c materials above and below T_c have not yet been

reported due to various difficulties. Also their superconducting properties are extremely sensitive to composition, such as oxygen stoichiometry. Moreover, since the superconducting coherence length is extremely short in these materials, one is not sure about the sample homogeneity even in small single crystals.

An alternative way to obtain information on the anisotropic elastic properties of these high T_c materials is to make measurements on samples with preferentially aligned crystallites, or the so-called sinterforged samples. Large size samples are rather easy to obtain in this form as compared to single crystals and pulsed echoes in ultrasonic experiments can be seperated owing to proper size of the samples. Oxygen content is usually more homogeneous because of the small size of the crystallites within them. Above all, these samples yield a nearly uniaxial symmetry, whereby the behaviour in the Cu–O layers, as opposed to directions perpendicular to them, can be sorted out.

Even though elastic properties have been investigated thoroughly and elastic constants determined accurately for many of them, no serious attempt has been made so far to plot elastic wave surfaces and study elastic anisotropy in these materials in a systematic way. In this paper we make an attempt to do this and analyse the results obtained on three of the popular high T_c superconductors, $Bi_2Sr_2CaCu_2O_{8-\delta}$, $RBa_2Cu_3O_{7-\delta}$ (R = Y or Gd) and $La_{2-x}Sr_xCuO_{4-\delta}$.

2. Elastic wave surfaces of selected high T_c superconductors

This is an attempt to study the temperature dependence of the anisotropy of elastic properties by plotting the phase velocity surfaces at temperatures above and below T_c for the three superconducting systems mentioned above. The phase velocity surface depicts the phase velocity ($v_p = \omega/k$) as a function of propagation direction and is independent of ω. The surfaces have been plotted either for single crystals, sinterforged samples or ceramic polycrystalline samples at temperatures above and below T_c depending upon the availability of elastic constant data.

All the three systems studied belong either to the orthorhombic or tetragonal symmetry with 9 and 6 elastic constants respectively. The elastic constant matrix for these two symmetry classes are

$$\begin{vmatrix} C_{11} & C_{12} & C_{13} & 0 & 0 & 0 \\ C_{12} & C_{22} & C_{23} & 0 & 0 & 0 \\ C_{13} & C_{23} & C_{33} & 0 & 0 & 0 \\ 0 & 0 & 0 & C_{44} & 0 & 0 \\ 0 & 0 & 0 & 0 & C_5 & 0 \\ 0 & 0 & 0 & 0 & 0 & C_{66} \end{vmatrix} \quad \text{and} \quad \begin{vmatrix} C_{11} & C_{12} & C_{13} & 0 & 0 & 0 \\ C_{12} & C_{11} & C_{13} & 0 & 0 & 0 \\ C_{13} & C_{13} & C_{33} & 0 & 0 & 0 \\ 0 & 0 & 0 & C_{44} & 0 & 0 \\ 0 & 0 & 0 & 0 & C_{44} & 0 \\ 0 & 0 & 0 & 0 & 0 & C_{66} \end{vmatrix}$$

respectively.

For a direction specified by the direction cosines l, m and n three bulk waves, viz, pure shear, quasi-shear and quasi-longitudinal can be propagated with velocities (v) and polarizations (u_j) determined by the Christoffel equations [1]

$$\left(\lambda_{ij} - \rho v^2 \delta_{ij}\right) u_j = 0 \quad (i, j = 1, 2, 3).$$

For orthorhombic symmetry, the λ's in the Christoffel equations are given by

$$\begin{aligned}
\lambda_{11} &= l^2 C_{11} + m^2 C_{66} + n^2 C_{55}, \\
\lambda_{22} &= l^2 C_{66} + m^2 C_{22} + n^2 C_{44}, \\
\lambda_{33} &= l^2 C_{55} + m^2 C_{44} + n^2 C_{33}, \\
\lambda_{12} &= lm(C_{12} + C_{66}), \\
\lambda_{13} &= ln(C_{13} + C_{55}), \\
\lambda_{23} &= mn(C_{44} + C_{23}),
\end{aligned} \tag{1}$$

whereas for tetragonal symmetry, with 6 constants, these parameters get modified to

$$\begin{aligned}
\lambda_{11} &= l^2 C_{11} + m^2 C_{66} + n^2 C_{44}, \\
\lambda_{22} &= l^2 C_{66} + m^2 C_{11} + n^2 C_{44}, \\
\lambda_{33} &= (l^2 + m^2) C_{44} + n^2 C_{33}, \\
\lambda_{12} &= lm(C_{12} + C_{66}), \\
\lambda_{13} &= ln(C_{13} + C_{44}), \\
\lambda_{23} &= mn(C_{44} + C_{13}).
\end{aligned} \tag{2}$$

The wave velocities of the three types of elastic wave fronts are then obtained for the *ab*, *ac* and *bc* planes as the eigen values of the Christoffel equations, which are then plotted as a function of propagation direction.

The work done on the three systems are separately outlined in the following sections.

2.1. $Bi_2Sr_2CaCu_2O_{8-\delta}$ (BSCCO):

This compound is the second member of the superconductor family having the general formula $Bi_2Sr_2Ca_{n-1}Cu_nO_{4+2n-\delta}$ with n = 1, 2, 3. The structure of BSCCO is orthorhombic with c = 30.8445 Å which is much larger than the lattice parameters a = 5.4091 Å and b = 5.4209 Å which are nearly equal.

Even though there are many reports on the elastic properties of this material, none of them gives the complete set of elastic constants, numbering nine, even at room temperature. The major work in this regard is by Wu *et al* [2] who have determined the temperature variation of several of the constants by ultrasonic measurements, but do not give all constants even at room temperature. There are other reports also which give only one or two constants [3–5].

However, a clear picture of the anisotropy in elastic wave propagation and its variation with temperature can be obtained since Saunders *et al* [6] have determined all the elastic constants from ultrasonic measurements on a textured sample of BSCCO both above and below T_c. In this sample, a high proportion of the grains are found to be aligned preferentially with the *c*-axis along the forging direction, while it is isotropic in the plane normal to the forging axis. So the sample is assumed to have a cylindrical symmetry and the five independent elastic constants are given at 290 K and 20 K. In addition, they have plotted the velocity surfaces for the *ac* plane at 290 K. Another important work in this direction is by Boekholt *et al* [7], who have reported room temperature elastic constants measured from Brillouin light scattering experiments on a single crystal. Here also cylindrical symmetry is assumed and five independent elastic constants have been determined. Both the data are tabulated in Table 1.

Table 1. Elastic constants of BSCCO (values in GPa).

C_{11}	C_{33}	C_{44}	C_{66}	C_{12}	C_{13}	T(K)	References
118.5	44.2	19.0	37.70	43.1	7.3	290	[6]
124.0	45.2	20.2	40.20	43.7	7.5	20	[6]
125.2	75 8	15.8	23.15	78.9	56.0	300	[7]

We have computed the wave velocity surfaces above and below T_c as the eigen values of the Christoffel equations using the elastic constants reported by Saunders *et al* [6].

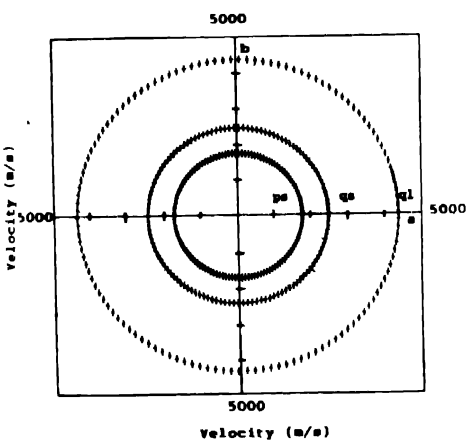

Figure 1(a). Wave velocity surfaces in the *ab* plane at 290 K for sinterforged BSCCO. *ps*, *qs* and *ql* represent the pure-shear, quasi-shear and quasi-longitudinal modes respectively.

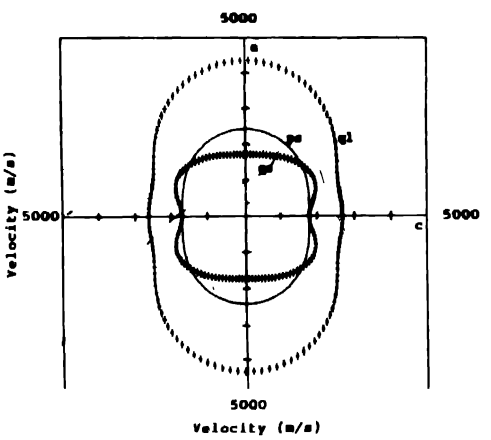

Figure 1(b). Wave velocity surfaces in the *ac*(*bc*) plane at 290 K for sinterforged BSCCO.

Because of the cylindrical symmetry of the sample, the surfaces are the same in the *ac* and *bc* planes. Figures 1(a) and 1(b) gives the plots at 290 K while Figures 1(c) and 1(d) are

those at 20 K where the symbols *ps*, *qs* and *ql* represent the pure-shear, quasi-shear and quasi-longitudinal modes respectively.

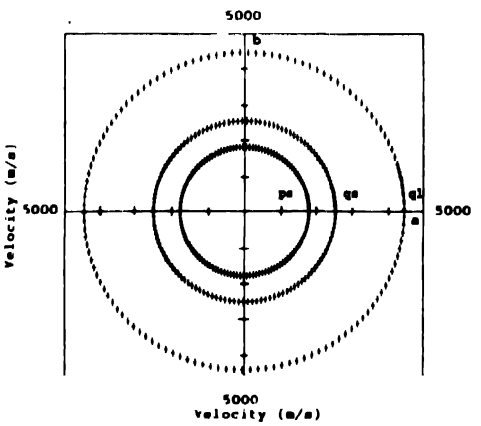

Figure 1(c). Wave velocity surfaces in the *ab* plane at 20 K for sinterforged BSCCO.

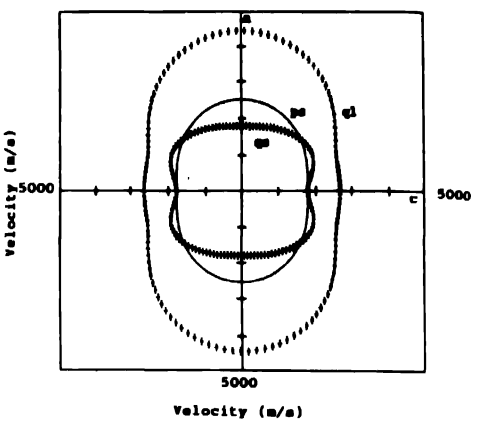

Figure 1(d). Wave velocity surfaces in the *ac*(*bc*) plane at 20 K for sinterforged BSCCO.

2.2. $RBa_2Cu_3O_{7-\delta}$ (RBCO) (R = Y or Gd) :

This compound is undoubtedly the most thoroughly investigated high T_c superconductor, owing to its relatively high T_c value and straight forward synthesis. The structure of RBCO at room temperature is orthorhombic. It is a tripled perovskite with a unit cell containing two Cu–O_2 layers (planes) and one Cu–O chain.

The elastic properties of this material have been investigated extensively. There exist several ultrasonic and other measurements of elastic constants on samples in the single crystal form [8–17]. The complete set of elastic constants reported by a selected number of workers is summarised in Table 2.

Table 2. Elastic constants of YBCO at 295 K (values in GPa).

C_{11}	C_{22}	C_{33}	C_{44}	C_{55}	C_{66}	C_{12}	C_{13}	C_{23}	References
231	268	186	49	37	95	132	71	95	[8]
223	244	138	61	47	97	37	89	93	[9]
230	230	150	50	50	85	100	100	100	[10]

Ming Lei *et al* [8] have measured the complete set of elastic constants by the resonant ultrasound technique, while Ledbetter and Lei [9] have given the complete set from a semi-theoretical estimate. The third set by Reichardt *et al* [10] is from inelastic neutron scattering and since they assume tetragonal symmetry only six constants are reported by them. Incomplete set of elastic constant data is available from many groups [11–17].

The wave velocity surfaces have been plotted at room temperature using the elastic constant data reported by Ming Lei *et al* [8]. Results obtained for propagation in the *ab*, *ac* and *bc* planes are plotted in Figures 2(a), 2(b) and 2(c). Though there are a number of

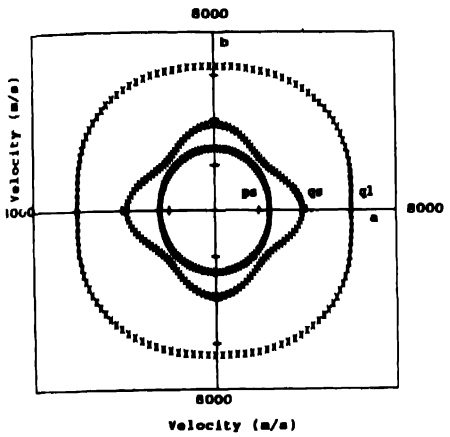

Figure 2(a). Wave velocity surfaces in the *ab* plane at room temperature for single crystal YBCO. *ps*, *qs* and *ql* represent the pure-shear, quasi-shear and quasi-longitudinal modes respectively.

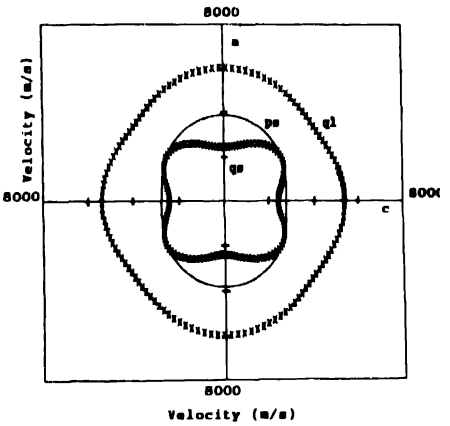

Figure 2(b). Wave velocity surfaces in the *ac* plane at room temperature for single crystal YBCO.

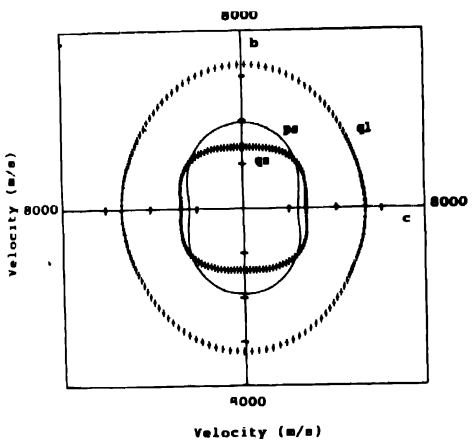

Figure 2(c). Wave velocity surfaces in the *bc* plane at room temperature for single crystal YBCO

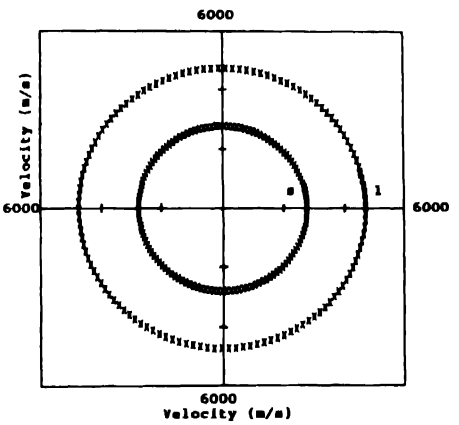

Figure 2(d). Wave velocity surfaces for polycrystalline GdBCO at 300 K. *s* and *l* represent the shear and longitudinal modes respectively.

measurements reported at low temperatures, for example Golding *et al* [12] give two constants C_{11} and C_{33} measured at 80 K, no data with complete set of elastic constants at low temperatures could be found.

As mentioned earlier, one of the alternative ways to shed light on the anisotropic nature of the elastic properties of these materials is to study the sinterforged materials when data on single crystals is lacking. Sinterforged YBCO samples show preferential

orientation [18] with 80% of the c-axis of the crystallites aligned within 20° of the forging axis. Since in the direction perpendicular to the forging axis, the a and b axes of the crystallites are randomly oriented, such samples show rotational symmetry and hence there are five different propagation modes for elastic waves. The major works are by Xu *et al* [19] and Zhao *et al* [20] who have reported incomplete sets of elastic constants at room temperature but no data at low temperatures could be found in literature for these types of samples.

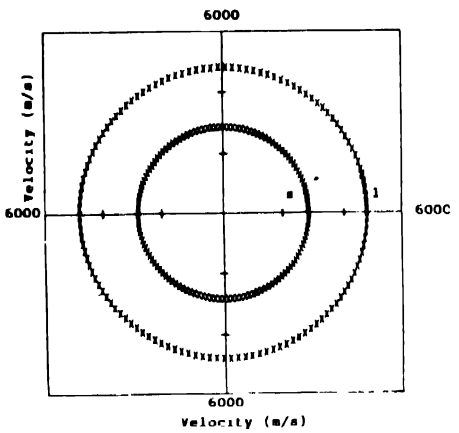

Figure 2(e). Wave velocity surfaces for polycrystalline GdBCO at 90 K.

Since a comparison of the wave surfaces above and below T_c has not been possible for YBCO due to the lack of data at low temperatures, we have plotted the surfaces for the polycrystalline '123' samples. For a polycrystalline material, the phase velocity is independent of direction and has only two values; v_l for the longitudinal wave and v_s for the shear wave. Many reports can be found in literature which give the longitudinal and transverse velocities of 123 compounds. The elastic constants taken from some of these reports [22–24] are tabulated in Table 3 along with the values we have measured for a superconducting GdBCO at 300 K and 90 K using the ultrasonic pulse echo overlap technique [21]. Figures 2(d) and 2(e) depict the surfaces at 300 K and 90 K plotted using the values measured by us where the symbols s and l represent the shear and longitudinal modes respectively.

Table 3. The longitudinal (C_l) and shear (C_s) elastic constants of polycrystalline GdBCO (values in GPa).

C_l	C_s	T(K)	References
143.5	49.4	300	[22]
149.1	52.4	90	[22]
158.2	52.0	–	[23]
170.6	64.5	4	[24]

2.3. $La_{2-x}Sr_xCuO_{4-\delta}$ (LSCO):

This superconducting compound is derived from the stoichiometric compound La_2CuO_4 (LCO) by replacing La^{3+} with Sr^{2+} (or Ba^{2+}) partially. The parent LCO is a semiconductor which exhibits tetragonal symmetry of *I4/mmm* space group at high temperatures (above 530 K), which distorts to a lower symmetry orthorhombic state on cooling. Since most of the measurements reported are at and below room temperature, the structure is invariably orthorhombic in all these. As La^{3+} is replaced by Sr^{2+}, the doping on the cation lattice introduces holes into the conduction band. The tetragonal-orthorhombic transition temperature decreases upon doping, the typical value being ≈ 180 K for $x = 0.15$. So the superconducting LSCO has a tetragonal structure at room temperature and it transforms to the orthorhombic state at ≈ 180 K.

Though the parent compound LCO is not a superconductor, the elastic properties of this compound have also been measured. Migliori *et al* [25] have measured all the nine constants at three different temperatures using the resonant ultrasound technique. Allan and Mackrodt [26] also give the complete set at room temperature which is the result of a molecular dynamics simulation. Incomplete data is available from different groups [27,28]. The complete set of elastic constants are tabulated in Table 4.

Table 4. Elastic constants of LCO (values in GPa).

C_{11}	C_{22}	C_{33}	C_{44}	C_{55}	C_{66}	C_{12}	C_{13}	C_{23}	T(K)	References
172.2	171.6	200	65.2	65.8	97.1	89.2	72.8	73.2	310	[25]
171.9	171.2	200	65.6	65.8	96.8	90.4	72.2	73.1	297	[25]
168.8	166.8	200	70.5	66 0	103.6	100.0	71.4	72.8	44	[25]
199.0	184.0	190	65.0	64.0	66.0	65.0	65.0	70.0	298	[26]

The velocity surface plots for LCO, given in Figures 3(a–c) represent the surfaces at 297 K for wave propagation in the *ab*, *ac* and *bc* planes respectively. The surfaces are more or less the same at 44 K and so the figures are not shown here.

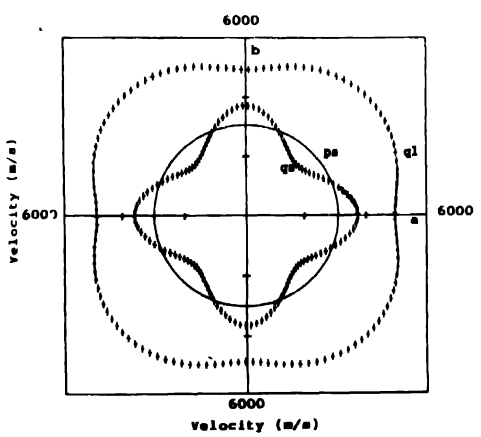

Figure 3(a). Wave velocity surfaces in the *ab* plane at 297 K for single crystal LCO. *ps*, *qs* and *ql* represent the pure-shear, quasi-shear and quasi-longitudinal modes respectively.

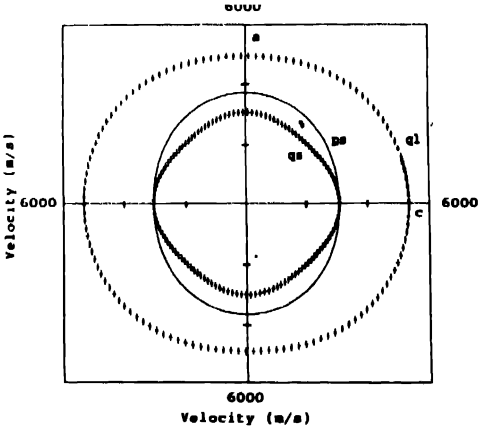

Figure 3(b). Wave velocity surfaces in the *ac* plane at 297 K for single crystal LCO.

Superconducting LSCO has a tetragonal structure at room temperature, with space group D_{4h}^{17}, and transforms into an orthorhombic state at 180 K with further structural anomalies on approach of the superconducting transition. Eventhough the first member of the high T_c superconductor family, data is comparatively less on LSCO compared to other superconductors. Migliori *et al* [29] have reported the complete set of elastic constants at 297 K measured using the resonant ultrasound technique. However, no data could be found which give all the six independent elastic constants at temperatures around or below T_c. The data which could be found in literature [29,30] are given in Table 5.

Table 5. Elastic constants of LSCO (values in GPa).

C_{11}	C_{33}	C_{44}	C_{66}	C_{12}	C_{23}	T(K)	References
248.0	205.0	67.4	58.3	48	65	297	[29]
263.4	246.5	–	–	–	–	50	[30]

Figures 3(d) and 3(e) give the velocity surfaces plotted for wave propagation in the *ab* and *ac* (*bc*) planes respectively for LSCO at 297 K using the elastic constants reported

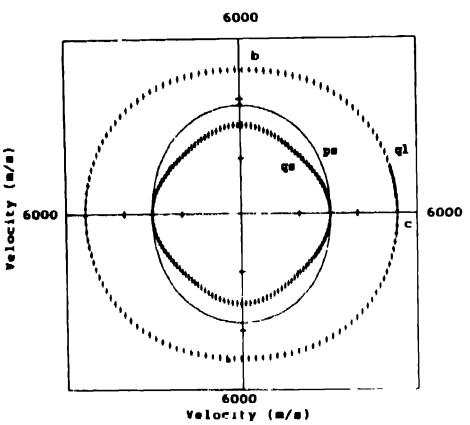

Figure 3(c). Wave velocity surfaces in the *bc* plane at 297 K for single crystal LCO.

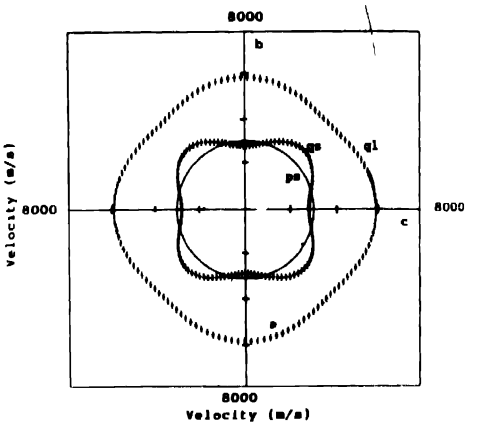

Figure 3(d). Wave velocity surfaces in the *ab* plane at room temperature for single crystal LSCO.

by Migliori *et al* [29]. Though there are many reports on the temperature variation of sound velocity, the absolute values of longitudinal and transverse velocities at two temperatures (one above and the other below T_c) could not be found for the same sample and hence the velocity surfaces below T_c are not plotted for polycrystalline LSCO.

3. Discussion and conclusion

The velocity surfaces plotted for the superconducting compounds for the propagation of elastic waves in different planes clearly depict the elastic anisotropy in these materials.

For BSCCO, the three surfaces for the shear, quasi-shear and quasi-longitudinal waves are circles in the *ab* plane (Figure 1(a)) indicating that the phase velocity is

independent of direction for all the waves. The compound possesses a layer structure which consists of adjacent pairs of Bi–O planes that alternate along the *c*-axis with pervoskite like multilayers. The Bi_2O_2 layers consist of two parallel, planar Bi–O sheets while the pervoskite multilayers comprise two Cu–O sheets in the form of corner sharing CuO_5 pyramids separated on the base sides by Ca ions. Crystals of BSCCO compounds have a mica-like morphology which indicates that the interlayer binding forces are very weak, while strong interatomic binding forces exist within the Cu–O planes.

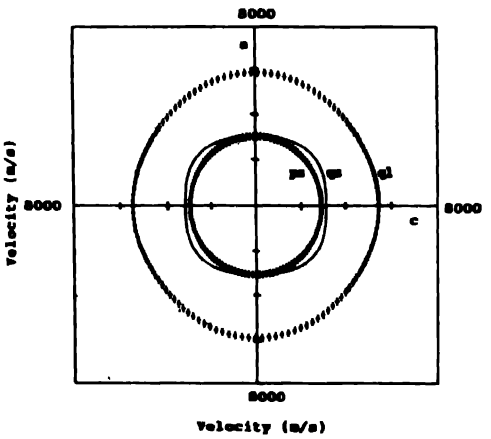

Figure 3(e). Wave velocity surfaces in the *ac*(*bc*) plane at room temperature for single crystal LSCO.

The direction independent velocities in the *ab* plane may be explained on the basis of the structure. It is possible that the strong interatomic forces within the Cu–O layers are responsible for the *ab* plane rigidity and therefore control the wave propagation within this plane so that these waves have velocities which are essentially independent of direction. In the *ac* (*bc*) plane, the wave surfaces plotted for the three waves clearly indicate the anisotropy in this plane. The velocity of the longitudinal elastic wave propagated within the layer *i.e.* along *a* (*b*) direction is much greater than that of the wave propagated along the *c* direction. The shear waves also have more or less the same behaviour. This behaviour is consistent with weak interlayer binding forces mentioned earlier.

The nature of the wave surfaces in YBCO should be similar to those in BSCCO since YBCO also possesses a layer structure. The unit cell of YBCO consists of two $Cu–O_2$ planes and one Cu–O chain with the Cu atoms located at two inequivalent positions. The first, Cu(2) has a pyramidal coordination while the Cu(1) located at the origin has a square planar coordination in which the near square Cu–O units share one corner and form chains along the *b* axis of the unit cell. The Cu(2) atoms are strongly bonded to the four oxygen atoms O(2) and O(3) forming the basis of the pyramid and are weakly bonded to the oxygen atom O(1) at the apex. Because of these features, there exists in the structure, two dimensional layers of Cu and O almost perpendicular to the *c* axis.

Just like BSCCO, the anisotropy is more in the *ac* and *bc* planes compared to the *ab* plane as is clear from Figures 2(a–c), though the velocities for the different modes are not independent of direction in the *ab* plane. In the *ac* plane the velocities are higher along the *c* direction. In other words, the elastic waves propagating within the layers are faster than those perpendicular to the layer or in the direction of weak coupling which is again similar to that of BSCCO. The nature of the wave surfaces in the *bc* plane is more or less similar to that in the *ac* plane since both *a* and *b* axes are within the layer and the *c* axis normal to the layer.

Comparing BSCCO and YBCO it can be found that BSCCO is more anisotropic. For example, the longitudinal velocity along the *a* axis is nearly double of that along the *c* axis in BSCCO while the ratio of velocities along *a* and *c* axes is not that high. This may be due to the larger number of layers present in the unit cell of BSCCO.

Though a nonsuperconductor, the interest in the elastic properties of LCO lies in the fact that the Cu–O planes present in the compound produce anisotropic elastic effects just as in a superconductor. Moreover, elastic and specific heat anomalies appear in this material at temperatures near T_c in the superconductor LSCO [31].

It is interesting to note that the anisotropy is more in the *ab* plane for both LCO and LSCO, contrary to what has been seen in the other two superconductors. The Cu–O perovskite layers perpendicular to the *c* axis are present in these materials also, which are separated by La/Sr–O_2 planes with a rock salt type of arrangement. Each O atom of the perovskite layers O(2) is bonded to two Cu atoms in the same plane and to four R atoms (R = 0.925 La + 0.075 Sr in LSCO and La in LCO) in adjacent planes, while each O atom of the rock salt layers O(1) is linked to five R atoms and one Cu atom in a distorted octahedral configuration. In other words, the R atoms are strongly bonded to both the O atoms located on the same plane and those of the perovskite layers and the nature of the atoms forming R can strongly influence the Cu–O bonding [32]. So it is likely that the wave propagation in the *ab* plane is not controlled by interatomic bonds within the layer alone, as in the case of the other two superconductors, but the La/Sr–O_2 bonds also have some influence on the wave propagation in this plane. So the combined influence of these two interatomic bonds may be responsible for the anisotropy in this plane as is clear from the Figures 3(a) and 3(d).

Comparing LCO and LSCO it is seen that velocities are higher in LSCO which indicate that doping with Sr makes the material stiffer. This is contrary to the usual trend where charge carriers are found to soften elastic waves by screening. This stiffening has been attributed to the suppressed onset of the low temperature orthorhombic phase in the doped material [29].

Not much information can be expected to be obtained regarding the anisotropy by plotting the wave surfaces for polycrystalline samples for which just two elastic constants exist. However, for the 1-2-3 compounds, the velocity surfaces have been plotted at two temperatures in order to check for any relative variations in the two velocity surfaces above

and below T_c. It is found that the curves are exactly similar at these two temperatures indicating that there is no relative changes in velocity as the sample undergoes a superconducting transition. In the case of the velocity surfaces obtained above and below T_c for the sinterforged BSCCO sample also, the wave surfaces are quite similar at the two temperatures. These results indicate that the anisotropic nature of wave propagation does not change significantly upon superconducting transition.

Acknowledgment

Work is supported by the Department of Science and Technology, Government of India. One of the authors (MSK) thanks the University Grants Commission for a fellowship.

References

[1] B A Auld in *Acoustic Fields and Waves in Solids* **Vol. 1** (New York : John Wiley & Sons) (1973)

[2] J Wu, Y Wang, P Guo, H Shen, Y Yan and Z Zhao *Phys. Rev.* **B47** 2806 (1993)

[3] J Wu, Y Wang, H Shen, J Zhu, Y Yan and Z Zhao *Phys. Lett.* **A148** 127 (1990)

[4] P Baumgart, S Blumenroder, A Erle, B Hillebrands, P Splittgeiber, G Guntherodt and H Schmidt *Physica* **C162-164** 1073 (1989)

[5] M Saint-Paul, J L Tholence, H Noel, J C Levet, M Potel and P Gougeon *Physica* **C166** 405 (1990)

[6] G A Saunders, C Fanggao, L Jiaqiang, Q Wang, M Cankurtaran, E F Lambson, P J Ford and D P Almond *Phys. Rev.* **B49** 9862 (1994)

[7] M Boekholt, J V Harzer, B Hillebrands and G Guntherodt *Physica* **C179** 101 (1991)

[8] Ming Lei, J L Sarrao, W M Visscher, T M Bell, J D Thompson and A Migliori *Phys. Rev.* **B47** 6154 (1993)

[9] H Ledbetter and M Lei *J. Mater. Res.* **6** 2253 (1991)

[10] W Reichardt, L Pintschovius, B Hennion and F Collin *Supercond. Sci. Tech.* **1** 173 (1988)

[11] P Baumgart, S Blumenroder A Erle, B Hillebrands, G Guntherodt and H Schmidt *Solid State Commun.* **69** 1135 (1989)

[12] B Golding, W H Haemmerle, L F Schneemeyer and J V Waszczak in *IEEE Ultrasonic Symp. Proc.* ed B R Mc Avoy (IEEE, Piscataway) p 1079 (1988)

[13] M Saint-Paul, J L Tholence, H Noel, J C Levet, M Potel and P Gougeon *Solid State Commun.* **69** 1161 (1989)

[14] M Saint-Paul and J Henry *Solid State Commun.* **72** 685 (1989)

[15] E Zouboulis, Sudha Kumar, U Welp, C H Chen, S K Chan, M Grimsdtch, J Downey and L Mc Neil *Physica* **C190** 329 (1992)

[16] T J Kim, J Kowalewski, W Assmus and W Grill Z *Phys.* **B78** 207 (1990)

[17] H C Gupta *Mod. Phys. Lett.* **B2** 811 (1988)

[18] Q Robinson, P Georgopoulos, D L Johnson, H O Marcy, C R Kannewurf, S J Hwu, T J Marks, K R Poeppelmeier, S N Song and J B Ketterson *Adv. Ceram. Mater.* **2** 380 (1987)

[19] M -F Xu, Y J Qian, K J Sun, Y Zheng, Q Ran, D Hinks, B K Sarma and M Levy *Physica* **B165-166** 1281 (1990)

[20] A Zhao, S Adenwalla, A Moreau, J B Ketterson, Q Robinson, D L Johnson, S -J Hwu, K R Poeppelmeier, M -F Xu, Y Hong, R F Wiegert, M Levy and B K Sarma *Phys. Rev.* **B39** 721 (1989)

[21] E P Pappadakis in *Physical Acoustics* **Vol.XII** eds. W P Mason and R N Thurston (New York : Academic) (1976)

[22] M S Kala, R Sreekumar, J Philip and N C Mishra *Phys. Stat. Solidi b* (in press)

[23] M Canlaurtaran, G A Saunders, D P Almond, A Al-Kheffaji, E F Lambson and R C Draper *J. Phys* C1 9067 (1989)

[24] D P Almond, Q Wang, J Freestone, E F Lambson, B Chapman and G A Saunders *J. Phys.* C 1 6853 (1989)

[25] A Migliori, W M Visscher, S E Brown, Z Fisk, S -W Cheong, B Alten, E T Ahrens, K A Kubat-Martin, J D Maynard, Y Huang, D R Kirk, K A Gillis, H K Kim and M H W Chan *Phys. Rev.* **B41** 2098 (1990)

[26] N L Allan and W C Mackrodt *Mater. Res. Soc. Symp. Proc* **99** 797 (1988)

[27] N V Zavaritsky, A V Samoilov, A A Yurgens, V S Klochko and V I Makarov *Physica* **C162-164** 562 (1989)

[28] N G Burma, A L Gaiduk, S V Zherlitsyn, I S Kolobov, V D Fil', A S Panfilov, I V Svechkarev, A P Ges', S N Barilo and D I Zhigunov *Fiz. Nizk. Temp.* **18** 247 (1992)

[29] A Migliori, W M Visscher, S Wong, S'E Brown, I Tanaka, H Kojima and P B Allen *Phys. Rev. Lett* **64** 2458 (1990)

[30] M Nohara, T Suzuki, Y Maeno, T Fujita, I Tanaka and H Kojima *Physica* **C185-189** 1397 (1991)

[31] J D Maynard and M J Mckenna in *Physical Acoustics* **Vol. XX** ed M Levy (San Diego Academic) (1992)

[32] A Santoro in *High Temperature Superconductivity* ed by J W Lynn (New York : Springer-Verlag) (1990)